11th World Congress on Computational Mechanics (WCCM XI)
5th European Conference on Computational Mechanics (ECCM V)
6th European Conference on Computational Fluid Dynamics (ECFD VI)
E. Oñate, J. Oliver and A. Huerta (Eds)

PREDICTION OF WHEEL AND RAIL PROFILE WEAR ON COMPLEX RAILWAY NETS

Alice Innocenti[1], Lorenzo Marini[1], Enrico Meli[1], Giovanni Pallini[1] and Andrea Rindi[1]

[1] Florence University, via di S. Marta 3 Florence Italy, www.unifi.it

Key words: Wheel and rail wear, Multibody modelling, Railway vehicles

Abstract. The prediction of wheel and rail wear is a fundamental issue in the railway field, both in terms of vehicle stability and in terms of economic costs (wheel and rail profile optimization from the wear viewpoint and planning of maintenance interventions). In this work the Authors present a model for the evaluation of the wheel and rail profile evolution due to wear specially developed for complex railway networks. The model layout is made up of two mutually interactive but separate units: a vehicle model for the dynamical analysis and a model for the wear evaluation. To study complex railway lines the Authors have developed a new statistical approach for the railway track description in order to achieve general significant accuracy results in a reasonable time. The wear model has been validated in collaboration with Trenitalia S.P.A and Rete Ferroviaria Italiana (RFI), which have provided the technical documentation and the experimental data relating to some tests performed on a scenery that exhibits serious problems in terms of wear: the vehicle *DMU ALn 501 Minuetto* circulating on the Aosta-Pre Saint Didier Italian line.

1 Introduction

In literature many important research works regarding the wear estimation can be found [1, 2]. However a substantial lack is present in the literature concerning wear models specially developed for complex railway network applications. In this case the computational load needed to carry out the exhaustive simulation of vehicle dynamics and wear evaluation turns out to be absolutely too high for each practical purpose. To overcome this critical issue of the wear prediction models, the Authors propose a new track statistical approach; more specifically it is suggested to replace the entire railway network with a discrete set of N_c different curved tracks (classified by radius, superelevation and traveling speed) statistically equivalent to the original network. The new approach allows a substantial reduction of the computational load and, at the same time, assures a good compromise in terms of model accuracy.

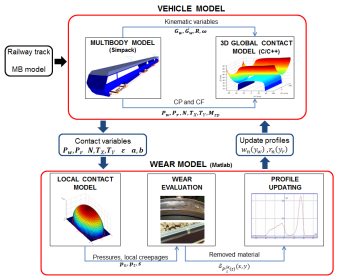

Fig. 1: General architecture of the model.

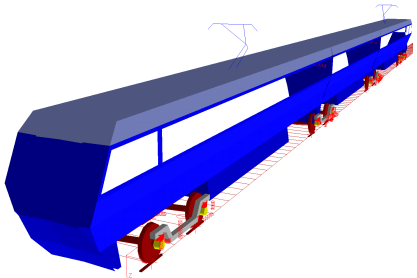

Fig. 2: Global multibody model view.

2 General Architecture of the Model

The layout of the model developed for studying the wear phenomena on complex railway lines is made up of two main parts: the *vehicle model* and the *wear model* (see Fig. 1). The *vehicle model* consists of the multibody model of the benchmark railway vehicle and the 3D global contact model that, during the dynamical simulation, interact directly online creating a loop. At each time integration step the first one evaluates the kinematic variables (position, orientation and their derivatives) relative to each wheel - rail contact pair and the second one, starting from the kinematic quantities, calculates the global contact variables (contact points and contact forces, contact areas and global creepages) [3, 4]. In the wear estimation research activities the track description is a critical task due to the complexity of the railway networks: to overcome these limitations, a new statistical approach has been developed to achieve general significant results in a reasonable time. The *wear model* is made up of three distinct phases: the local contact model, the wear evaluation and the profile update. The local contact model, starting from the global contact variables, estimates the local contact pressures and creepages inside the contact patch and detects the creep zone of the contact area [4]. Subsequently the distribution of removed material is calculated both on the wheel and on the rail surface only within the creep area by using an experimental relationship between the removal material and the energy dissipated by friction at the contact interface [1]. Finally the wheel and rail worn profiles are derived from the original ones through an appropriate innovative update strategy. The new updated wheel and rail profiles (one mean profile both for all the wheels of the vehicle and for all the rails of the considered tracks) are then fed back as inputs to the *vehicle model* and the whole model architecture can proceed with the next discrete step. The evolution of the wheel and rail profiles is therefore a discrete process. The choice of the discrete step for the profiles updates as it will be clarified in the following, has to consider the difference between the time scales characterizing the wheel and rail wear evolution rates.

3 The Vehicle Model

The benchmark vehicle investigated for this research is the *DMU Aln 501 Minuetto*, a passenger transport unit widespread in Italian Railways where is equipped with the stan-

dard ORE S1002 wheel profile and UIC60 rail profile canted at 1/20 rad. This particular vehicle exhibits in fact severe wear and stability problems mainly caused by the adopted matching. Its mechanical structure and its inertial, elastic and damping properties can be found in literature [5]. The multibody model (see Fig. 2) consists of several rigid bodies connected each other by means of appropriate elastic and damping elements; particularly the vehicle is equipped with two suspension stages. Both the stages of suspensions have been modeled by means of three-dimensional viscoelastic force elements taking into account all the mechanical non linearities of the system (bumpstop clearance, dampers and rod behaviour). In this research activity a specifically developed 3D global contact model has been used in order to improve reliability and accuracy of the contact points detection. In particular it is divided in two steps: the contact points detection algorithm is based on a classical formulation of the contact problem in multibody field and the its most innovative aspect is the reduction of the algebraic problem dimension (from 4D to a simple 1D scalar problem) through exact analytical procedures [3, 6]. Then the global contact forces and creepages are evaluated with Hertz's and Kalker's theories [4].

4 The Wear Model

4.1 The Local Contact Model

The wear model inputs are the global contact variables estimated by the vehicle model. Since a local wear computation is required, the global contact parameters need to be post-processed and it can be achieved through the simplified Kalker's theory implemented in the FASTSIM algorithm [4], capable to compute the local distribution of normal p_n and tangential $\mathbf{p}_t$ stresses and local creepages $\mathbf{s}$ across the wheel-rail contact area.

4.2 The Wear Evaluation

To evaluate the specific volume of removed material on wheel and rail due to wear $\delta_{P^j_{wi}(t)}(x,y)$ and $\delta_{P^j_{ri}(t)}(x,y)$ (where x and y indicate the coordinates of a generic point of the contact patch) related to the i-th contact points $P^j_{wi}(t)$ and $P^j_{ri}(t)$ on the j-th wheel and rail pair for unit of distance traveled by the vehicle (expressed in m), and for unit of surface (expressed in mm), an experimental relationship between the volume of removed material and the frictional work [1] has been used. More specifically, the local contact stresses $\mathbf{p}_t$ and creepages $\mathbf{s}$ are used to evaluate the *wear index* I_W (expressed in $\mathrm{N/mm^2}$), which represents the frictional power generated by the tangential contact pressures: $I_W = \mathbf{p}_t \bullet \mathbf{s}/V$ where V is the longitudinal velocity speed. This index can be correlated with the *wear rate* K_W, that is the mass of removed material (expressed in $\mu\mathrm{g/m\,mm^2}$) for unit of distance traveled by the vehicle and for unit of surface. The correlation is based on real data available in literature [1], which have been acquired from experimental wear tests carried out in the case of metal to metal contact with dry surfaces using a twin disc test arrangement. The experimental relationship between K_W and I_W adopted for the wear model described in this work is the following:

$$K_W(I_W) = \begin{cases} 5.3 * I_W & I_W < 10.4 \\ 55.1 & 10.4 \leq I_W \leq 77.2 \\ 61.9 * I_W - 4778.7 & I_W > 77.2. \end{cases} \quad (1)$$

Once the wear rate $K_W(I_W)$ is known (the same both for the wheel and for the rail), the specific volume of removed material on the wheel and on the rail (for unit of distance traveled by the vehicle and for unit of surface) can be calculated (expressed in $\mathrm{mm}^3/\mathrm{m}\,\mathrm{mm}^2$): $\delta_{P^j_{wi}(t)}(x,y) = K_W(I_W)\frac{1}{\rho}$, $\delta_{P^j_{ri}(t)}(x,y) = K_W(I_W)\frac{1}{\rho}$ where ρ is the material density.

4.3 The Profile Update Procedure

After obtaining the amount of worn material, wheel and rail profiles need to be updated to be used as the input of the next step of the whole model (further details can be found in literature [6]). Preliminarily some integration and average operations allow the evaluation of the average wear quantities $\overline{\Delta}^w(s_w)$, $\overline{\Delta}^r(s_r)$ needed to obtain as output of the wear model a single mean profile both for the wheel and for the rail (the introduction of the natural abscissas s_w and s_r of the curves $w(y_w)$ and $r(y_r)$ leads to a better accuracy in the calculation of the worn profiles).

At this point an average on the curved tracks is necessary when a statistical description of the track is adopted. Different wear distributions $\overline{\Delta}^w_k(s_w)$ and $\overline{\Delta}^r_k(s_r)$ for each of the N_c curve classes will be obtained from the previous steps (with $1 \leq k \leq N_c$). The statistical weigths of the curve classes p_k (see paragraph 5.2), calculated as the ratio between the track length characterized by the curve conditions related to the k-th class (in terms of radius and superelevation values) and the total railway track length, have to be introduced to consider the frequency with which each curve appears on the actual railway track. Consequently, for the statistical approach, the following ralations for the removed material hold: $\sum_{k=1}^{N_c} p_k \overline{\Delta}^w_k(s_w) = \overline{\Delta}^w_{stat}(s_w)$, $\sum_{k=1}^{N_c} p_k \overline{\Delta}^r_k(s_r) = \overline{\Delta}^r_{stat}(s_r)$ with $\sum_{k=1}^{N_C} p_k = 1$. Obviously, when the dynamic simulations are performed on the complete railway track the previous equations simply become $\overline{\Delta}^w(s_w) = \overline{\Delta}^w_{track}(s_w)$, $\overline{\Delta}^r(s_r) = \overline{\Delta}^r_{track}(s_r)$.

Since it normally takes traveled distance of thousands kilometers in order to obtain measurable wear effects, an appropriate scaling procedure is necessary to reduce the simulated track length with a consequent limitation of the computational effort. Hypothesizing the almost linearity of the wear model with the traveled distance inside the discrete steps, it is possible to amplify the removed material during the dynamic simulations by means of a scaling factor which increases the distance traveled by the vehicle. In this work adaptive discrete steps (function of the wear rate and obtained imposing the threshold values D^w_{step} and D^r_{step} on the maximum of the removed material quantity on the wheelsets and on the tracks at each discrete step) have been chosen to update the wheel and rail profiles (see eq. 2). The evaluation of the discrete steps for the profile updates, with the consequent scaling of $\overline{\Delta}^w_{stat}(s_w)$, $\overline{\Delta}^w_{track}(s_w)$ and $\overline{\Delta}^r_{stat}(s_r)$, $\overline{\Delta}^r_{track}(s_r)$, represents the major difference between the update strategy of wheel and rail:

1) the removed material on the wheel due to wear is proportional to the distance traveled by the vehicle; in fact a point of the wheel is frequently in contact with the rail in a

number of times proportional to the distance. If km_{tot} is the total mileage traveled by the considered vehicle, km_{step} is the length of the discrete step corresponding to the threshold value on the wear depth D^w_{step} and km_{prove} is the overall mileage traveled by the vehicle during the dynamic simulations, the material removed on the wheels and the corresponding km_{step} value have to be scaled according to the following laws:

$$\overline{\Delta}^w_{stat/track}(s_w)\frac{D^w_{step}}{\overline{D}^w_{stat/track}} = \overline{\Delta}^w_{stat/track}{}^{sc}(s_w), \quad km^{stat/track}_{step} = \frac{D^w_{step}}{\overline{D}^w_{stat/track}} km^{stat/track}_{prove}, \quad D^w_{stat/track} = \max_{s_w} \overline{\Delta}^w_{stat/track}(s_w); \tag{2}$$

The km_{prove} parameter assumes a different value according to the different way in which the track is treated: if the wear evolution is evaluated on the overall railway track (of length l_{track}) then $km^{track}_{prove} = l_{track}$ while, if the track statistical approach is considered, $km^{stat}_{prove} = l_{ct}$ is the mileage traveled by the vehicle during each of the N_c dynamic simulations. This consideration explains the deeply difference in terms of computational load between the two considered cases.

2) the depth of rail wear is not proportional to the distance traveled by the vehicle; in fact the rail tends to wear out only in the zone where it is crossed by the vehicle and, increasing the traveled distance, the depth of removed material remains the same. On the other hand the rail wear is proportional to the total tonnage M_{tot} burden on the rail and thus to the total vehicle number N_{tot} moving on the track. Therefore, if N_{step} is the vehicle number moving on the track in a discrete step, the quantity of rail removed material at each step will be:

$$\overline{\Delta}^r_{stat/track}(s_r)\frac{D^r_{step}}{\overline{D}^r_{stat/track}} = \overline{\Delta}^r_{stat/track}{}^{sc}(s_r), \quad N^{stat/track}_{step} = \frac{D^r_{step}}{\overline{D}^r_{stat/track}} N^{stat/track}_{prove}, \quad D^r_{stat/track} = \max_{s_r} \overline{\Delta}^r_{stat/track}(s_r); \tag{3}$$

where $N^{stat}_{prove} = N_c$ and obviously $N^{track}_{prove} = 1$.

Then an appropriate smoothing of the worn material distributions is required to avoid the numerical noise that affect the worn material distributions and finally the new profiles are obtained removing the worn material in the normal direction to the wheel and rail old profile respectively.

5 Railway Track Description

5.1 The Aosta Pre-Saint Didier Line

The whole Aosta-Pre Saint Didier railway network (characterized by an approximate length of $l_{track} \approx 31$km) has been reconstructed and modeled in the Simpack environment starting from the track data provided by RFI.

5.1.1 Wear Control Parameters and Experimental Data

The reference parameters FH (flange height), FT (flange thickness) and QR quota are capable of estimating the wheel profile evolution due to wear without necessarily knowing the whole profile shape (see Fig. 4) [7]. An additional control parameter QM is then introduced to evaluate the evolution of rail wear see Fig. 3). The experimental data provided

by Trenitalia have been measured for all the vehicle wheels on three different vehicles *Aln 501 Minuetto* operating on the Aosta-Pre Saint Didier track that are conventionally called DM061, DM068, DM082. The experimental data have been properly processed mediating on all the vehicle wheels to obtain as output a single average wheel profile and to reduce the measurement errors (see Tab. 2) [6]. Concerning the rail wear, the QM quota evolution is compared with a criterion present in literature [8]. A proportionality relationship between tonnage burden on the track and wear holds: a rail wear of 1 mm on the rail head height every $100Mt$ (millions of tons) of accumulated tonnage.

5.2 The Statistical Approach

The present section is an overview on the procedure used in deriving a significant statistical track description, an essential task to make possible and rationalize the approach and the simulation work on a complex railway line. In this work the statistical approach has been exploited to draw up a virtual track of the Aosta-Pre Saint Didier line [6]. The basic idea is to substitute the simulation on the whole track with an equivalent set of simulations on short curved tracks. The curve tracks are obtained dividing the whole track in n_{class} curve radius intervals $[R_{min} - R_{max}]$; each of these is furthermore divided in n_{class} superelevation subclasses $[h_{min} - h_{max}]$ (Tab. 1). For each radius class, a representative radius R_c is calculated as a weighted average on all the curve radii, using the length of the curve as weighting factor. Similarly for each superelevation subclass the correspondent representative superelevation H is chosen as a weighted average on all the curve superelevation, using the length of curve as a weighting factor. For each representative curve a speed value V is chosen as the minimum value between the maximum speed allowable in curve (equal to $V_{max} = 60\,\mathrm{km/h}$ and depending on the radius, the superelevation and the vehicle characteristics) and the speed $\tilde{V}$ calculated by imposing a non-compensated acceleration $a_{nc}^{lim} = 0.8\,\mathrm{m/s^2}$ [8]; for the straight class the speed value, obtained from the track data, is equal to $130\,\mathrm{km/h}$. Finally the weighting factor p_k is introduced for each subclass to take into account the frequency of a certain matching radius-superelevation in the track and to diversify the wear contributions of the different curves. By way of example in Tab. 1 is shown the data of the statistical analysis with $n_{class} = 7$.

6 Results

6.1 Simulation Strategy

The following specific algorithm has been adopted for updating the profiles according to different time scales that affect the wheel and rail wear evolutions [6]:
1) to have a good compromise between calculation times and result accuracy a suitable number of discrete steps both for the wheel and for the rail steps have been chosen, $n_{sw} = 20$ and $n_{sr} = 5$: consequently the wheel wear threshold D_{step}^{w} (see section 4.3) has been fixed equal to 0.2 mm and the value of the rail wear threshold D_{step}^{r} (see section 4.3) has been set equal to 0.8 mm to obtain an appreciable rail wear during the simulations.

Tab. 1: Data of the curvilinear tracks of the statistical analysis with $n_{class} = 7$.

$\mathbf{R}_{min}$ (m)	$\mathbf{R}_{max}$ (m)	**Superelevation** $h_{min} - h_{max}$ (mm)	$\mathbf{R}_c$ (m)	**H** (mm)	**V** (km/h)	$\mathbf{p}_k$ %
150	175	100 - 119	162	110	57	0.93
		120 - 140	162	131	60	1.30
175	209	80 - 99	195	90	60	7.09
		100 - 119	195	103	60	7.42
		120 - 140	195	126	60	5.48
209	259	60 - 79	237	70	60	0.87
		80 - 99	237	83	60	8.76
		100 - 119	237	109	60	4.63
		120 - 140	237	120	60	0.47
259	342	40 - 59	293	50	60	0.28
		60 - 79	293	65	60	3.05
		80 - 99	293	83	60	0.90
		100 - 119	293	100	60	0.31
342	503	40 - 59	376	49	60	1.13
		60 - 79	376	62	60	1.26
503	948	20 - 39	774	24	60	1.73
		40 - 59	774	40	60	0.42
948	8400	0 - 19	3572	5	60	2.40
		20 - 39	3572	20	60	0.91
8400	∞	0	∞	0	130	50.65

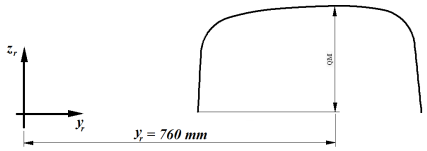

Fig. 3: Definition of rail wear control parameter.

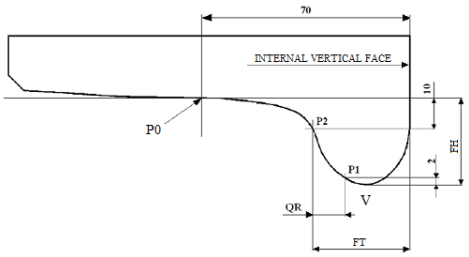

Fig. 4: Definition of the wheel wear control parameters.

Tab. 2: Experimental processed data.

Vehicle	**Distance traveled** (km)	**FH** (mm)	**FT** (mm)	**QR** (mm)
DM061	0	28.0	32.5	10.8
	1426	28.2	31.5	9.8
	2001	28.1	30.8	9.1
	2575	28.0	30.2	8.6
DM068	0	28.0	32.5	10.8
	1050	28.0	31.8	10.0
	2253	28.0	30.2	8.5
	2576	28.0	30.0	8.4
DM082	0	28.0	32.5	10.8
	852	28.0	32.3	10.6
	1800	28.0	31.3	9.6
	2802	28.0	30.3	8.7
	3537	27.6	30.0	8.3

2) the wear evolutions on wheel and rail have been decoupled because of the different scales of magnitude. While the wheel wear evolves, the rail is supposed to be constant: in fact, in the considered time scale, the rail wear variation is negligible. On the other hand the time scale characteristic of the rail wear evolution, much greater than the wheel wear evolution one, causes the same probability that each discrete rail profile comes in contact with each possible wheel profile: for each rail profile, the whole wheel wear evolution (from the original profile to the final profile) has been simulated.
Initially the wheel (starting from the unworn profile w_0^0) evolves on the unworn rail profile r_0 producing the discrete wheel profiles $w_0^0, w_1^0, ..., w_{n_{sw}}^0$ (step $p_{1,1}$). Then the virtual rail profiles $r_1^{(i+1)}$, obtained by means of the simulations (w_i^0, r_0), are arithmetically averaged so as to get the update rail profile r_1 (step $p_{1,2}$). This procedure can be repeated n_{sr} times in order to perform all the rail discrete steps (up to the step $p_{n_{sr},2}$).

6.2 Complete Aosta-Pre Saint Didier Railway Line Results

In this paragraph the results obtained studying the whole Aosta-Pre Saint Didier line will be presented and compared with the experimental data.

6.2.1 Evolution of Wear Control Parameters

The progress of FT dimension, for the n_{sr} discrete step of the rail, is shown in Fig. 5 as a function of the mileage; as it can be seen, the decrease of the dimension is almost linear with the traveled distance except in the first phases, where the profiles are still not conformal enough. The FH quota progress is represented in Fig. 6 and shows that, due to the high sharpness of the considered track and to the few kilometers traveled, the wheel wear is mainly localized on the flange rather than on the tread; therefore the flange height remains near constant in agreement with experimental data (see Tab. 2). The QR trend (Fig. 7) shows the almost linearly decrease of the flange steepness except in the first phases, leading to an increase of the conicity of the flange. Finally the evolution of the wheel control parameters remains qualitatively similar as the rail wear raises, with a slight increase of all the quotas that indicates a shift of the material removed towards the wheel tread, because of the more and more conformal contact (see also Tab. 3). The QM evolution for the analysis of the rail wear is presented in Fig. 8 and shows the almost linear dependence between the rail wear and the total tonnage burden on the track. The amount of removed material on the rail head, equal to 2.97 mm, is in agreement with the criterion present in literature [8] (1 mm on the rail head height every 100 Mt of accumulated tonnage); the whole simulation procedure corresponds to a tonnage of $M_{tot} = N_{tot} * M_v = 310\ Mt$ (the vehicle mass is $M_v = 104700$ kg) (see Tab. 4, 5).

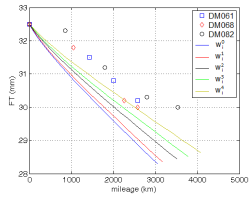

Fig. 5: Complete track: FT.

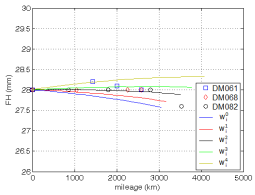

Fig. 6: Complete track: FH.

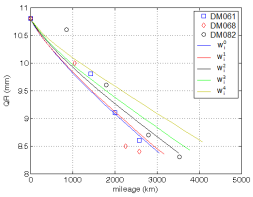

Fig. 7: Complete track: QR.

6.2.2 Evolution of the Wheel and Rail Profile

The wear evolution on the wheel profiles evolving on different rail steps is presented in the Fig. 9, 10 (for reasons of brevity only the profiles evolution related to the first and the last rail steps are represented). The figures show the main localization of the material removed on the wheel flange due to the quite sharp curves that characterize the Aosta-Pre Saint Didier line. In Fig. 11 the evolution of the rail profile is shown.

6.3 Statistical Analysis Results

A suitable value of the n_{class} parameter have to be supposed; for the Aosta-Pre Saint Didier line the value $n_{class} = 10$ represents a good compromise among track description, result accuracy and computational effort.

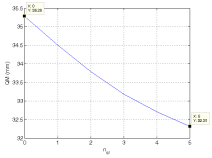

Fig. 8: Complete track: QM.

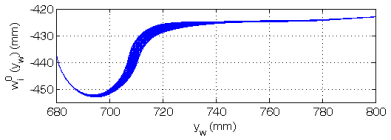

Fig. 9: Complete track: w_i^0.

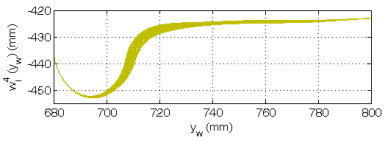

Fig. 10: Complete track: w_i^4.

6.3.1 Evolution of Wear Control Parameters

The Figures 12-14 present the evolution of the wear control parameters. It can be seen the same qualitatively trend obtained with the complex railway approach both concerning the conformity considerations and the localization of the worn material on the wheel flange (see also Tab. 3). QM progress lead to a reduction of the rail head height of 3.28 mm in agreement with the criterion present in literature (1 mm on the rail head height every 100 Mt of accumulated tonnage); in fact the whole simulation corresponds to a tonnage of $M_{tot} = N_{tot} * M_v = 322\ Mt$ (see Tab. 4, 5).

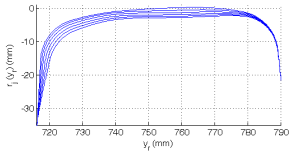

Fig. 11: Complete track: rail evolution.

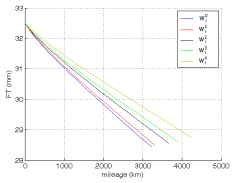

Fig. 12: Statistical track: FT.

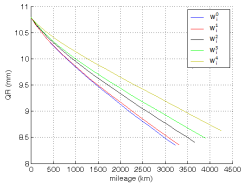

Fig. 13: Statistical track: QR.

6.3.2 Evolution of the Wheel and Rail Profile

The evolution of the wheel and rail profiles are qualitatively in agreement with the complete railway approach and the same considerations of section 6.2.2 hold (Fig. 15-17).

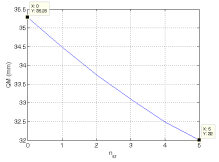

Fig. 14: Statistical track: QM.

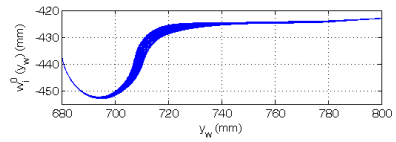

Fig. 15: Statistical track: w_i^0.

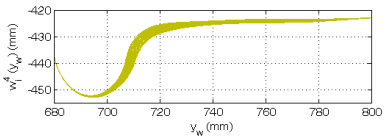

Fig. 16: Statistical track: w_i^4.

6.4 Complete Railway Line and the Statistical Analysis Comparison

A quantitatively comparison between the results obtained with the complete railway line and the statistical approach with $n_{class} = 10$ has been carried out. In Tab. 3 the final values of the wheel reference dimensions and the evolution of the total mileage km_{tot} for

all the n_{sr} rail step are presented. The flange height increase as the rail profile is more and more worn, together with the increase of the flange thickness, indicates a shift of the material removed towards the wheel tread due to the variations of the contact conditions as previously explained. In Tabs. 4-5 the comparison of the rail parameters is shown.

Tab. 3: Evolution of the wheel parameters.

	Complete Railway	**Statistical Description** $n_{class} = 10$	
	FH (mm)	FH (mm)	e (%)
km^0_{tot}	27.57	27.86	1.0
km^1_{tot}	27.73	27.98	0.9
km^2_{tot}	27.89	28.12	0.8
km^3_{tot}	28.07	28.27	0.7
km^4_{tot}	28.33	28.60	1.0
	FT (mm)	FT (mm)	e (%)
km^0_{tot}	28.30	28.43	0.5
km^1_{tot}	28.36	28.50	0.5
km^2_{tot}	28.44	28.56	0.4
km^3_{tot}	28.52	28.62	0.4
km^4_{tot}	28.63	28.75	0.4
	QR (mm)	QR (mm)	e (%)
km^0_{tot}	8.38	8.35	0.4
km^1_{tot}	8.35	8.36	0.1
km^2_{tot}	8.37	8.41	0.5
km^3_{tot}	8.43	8.48	0.6
km^4_{tot}	8.57	8.63	0.7
	km_{tot} (km)	km_{tot} (km)	e (%)
km^0_{tot}	3047	3219	5.6
km^1_{tot}	3163	3306	4.5
km^2_{tot}	3515	3659	4.1
km^3_{tot}	3772	3893	3.2
km^4_{tot}	4080	4244	4.0

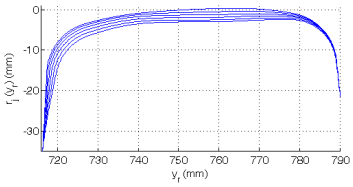

Fig. 17: Statistical track: rail evolution.

Tab. 4: Evolution of the QM quota.

Complete Railway	**Statistical Description** $n_{class} = 10$	
QM (mm)	QM (mm)	e (%)
32.31	32.00	0.6

Tab. 5: Total vehicle number N_{tot}.

	Complete Railway	**Statistical Description** $n_{class} = 10$	e (%)
N_{tot}	2957850	3076200	4.0

6.5 Sensibility Analysis of the Statistical Approach

A sensibility analysis of the statistical approach with respect to the class number n_{class} will be presented. The variation range studied is $n_{class} = 4 \div 10$. By analyzing the data relative to the wheel presented in Tab. 6 the trend of the wheel parameters shows an increase both of the wheel flange dimensions in according to the variation of the contact conditions explained in the previous sections (see 6.2-6.4). Analogously the km_{tot} evolution trend is the same for each of the statistical analysis considered, and also the mileage increases as the rail wear increases indicating the more and more conformal contact between wheel and rail surfaces. The error e, referred to the complete railway approach, shows less and less consistency between the results of the whole railway approach and the statistical analysis as the n_{class} parameter decreases (Tab. 6). The less model accuracy and the underestimation of the worn material as the track description is more and more rough is found also by analyzing the rail control parameters (Tab. 7).

Tab. 6: Evolution of the wheel control parameters.

Statistical Description		FH (mm)	e (%)	FT (mm)	e (%)	QR (mm)	e (%)	km_{tot} (km)	e (%)
$n_{class} = 4$	km^0_{tot}	26.99	2.1	28.02	1.0	8.29	1.0	3775	23.9
	km^1_{tot}	27.12	2.2	28.16	0.7	8.25	1.2	3967	25.4
	km^2_{tot}	27.26	2.3	28.19	0.9	8.28	1.1	4267	21.4
	km^3_{tot}	27.49	2.1	28.26	0.9	8.35	1.0	4521	19.9
	km^4_{tot}	27.71	2.2	28.35	1.0	8.47	1.2	4793	17.5
$n_{class} = 6$	km^0_{tot}	27.08	1.7	28.06	0.8	8.31	0.8	3620	18.8
	km^1_{tot}	27.24	1.7	28.18	0.6	8.28	0.9	3743	18.5
	km^2_{tot}	27.40	1.8	28.23	0.7	8.29	0.9	4038	14.9
	km^3_{tot}	27.62	1.6	28.31	0.8	8.36	0.9	4237	12.3
	km^4_{tot}	27.83	1.8	28.40	0.8	8.48	1.1	4569	12.0
$n_{class} = 8$	km^0_{tot}	27.14	1.6	28.10	0.7	8.33	0.6	3431	12.6
	km^1_{tot}	27.30	1.5	28.19	0.6	8.30	0.5	3529	11.6
	km^2_{tot}	27.47	1.5	28.26	0.6	8.31	0.7	3903	11.0
	km^3_{tot}	27.69	1.3	28.35	0.6	8.37	0.8	4092	8.5
	km^4_{tot}	27.90	1.5	28.44	0.7	8.49	0.9	4445	8.9
$n_{class} = 10$	km^0_{tot}	27.86	1.0	28.43	0.5	8.35	0.4	3219	5.6
	km^1_{tot}	27.98	0.9	28.50	0.5	8.36	0.1	3306	4.5
	km^2_{tot}	28.12	0.8	28.56	0.4	8.41	0.5	3659	4.1
	km^3_{tot}	28.27	0.7	28.62	0.4	8.48	0.6	3893	3.2
	km^4_{tot}	28.60	1.0	28.75	0.4	8.63	0.7	4244	4.0

Tab. 7: Rail control parameters evolution.

Statistical Description	QM (mm)	e (%)	N_{tot}	e (%)
$n_{class} = 4$	31.58	2.3	3797900	28.4
$n_{class} = 6$	31.69	1.9	3543500	19.8
$n_{class} = 8$	31.83	1.5	3309800	11.9
$n_{class} = 10$	32.00	1.0	3076200	4.0

Tab. 8: Processor and integrator data.

Processor	INTEL Xeon CPU X5560 2.80 GHz 24GB RAM	
Integrator	Type	ODE5
	Alghoritm	Dormand-Prince
	Order	5
	Step type	fixed
	Stepsize	10^{-4} s

6.6 Computational Effort Comparison

This section deal with the comparison between the computational load required by the different approaches considered in this work. The characteristics of the processor and the integrator parameters used are briefly reported in Tab. 8. The mean computational times relative to each discrete step of the whole model loop are schematically summarized in Tab. 9 (t_{wt}, t_{rt} are the total simulation time for wheel and rail, t_{wd} and t_{rd} the dynamical simulation times and t_{ww}, t_{rw} the wear simulation times). The huge computational effort

Tab. 9: Computational time.

Railway approach		Computational time: Wheel wear evaluation t_{wd}	t_{ww}	t_{wt}	Rail wear evaluation t_{rd}	t_{rw}	t_{rt}	Total simulation time t_T
Complete track		4d 12m	1d 38m	5d 50m	3dd 12h	1d 8h 40m	4dd 20h 40m	24dd 7h 20m
Statistical analysis	$n_{class} = 4$	8m	4m	12m	2h 40m	1h 20m	4h	20h
	$n_{class} = 6$	13m	6m	19m	4h 20m	2h	6h 20m	1d 7h 40m
	$n_{class} = 8$	18m	7m	25m	6h	2h 20m	8h 20m	1d 16h 40m
	$n_{class} = 10$	24m	10m	34m	8h	3h 20m	11h 20m	2dd 8h 40m

that affects the complete railway line simulation, makes this approach hardly feasible to the wear evolution studies typical of the railway field. On the contrary the statistical track description (see the Tab. 6, 7 and 9) shows a high saving of computational load and at the same time a not excessive loss of model accuracy.

7 Conclusions

The Authors have presented a complete model for the wheel and rail wear prediction in railway field specifically developed for complex railway nets where the exhaustive analysis

on the complete line is not feasible because of the computational load required. The most innovative aspect is the track statistical approach based on the replacement of the complete railway line with a statistically equivalent set of representative curved tracks. The whole model has been validated on a critical scenario in terms of wear in Italian railways. Particularly the new model results have been compared both with the complete railway network ones and with the experimental data provided by TI. If the track discretization is accurate enough, the developed model turned out to be quite in agreement both with the experimental data and with the complete railway network model, and the evolution of all the profile characteristic dimensions described in a satisfying way the wear progress both on wheel and rail. As regard to the track description, the statistical analysis turned out to be a good approach with a significant saving of computational time despite a very slight loss of the result accuracy if compared to the complete railway network model. Future developments will be based on further model validations through new experimental data always provided by TI and on a better investigation of the statistical approach.

REFERENCES

[1] F. Braghin, R. Lewis, R. S. Dwyer-Joyce, and S. Bruni. A mathematical model to predict railway wheel profile evolution due to wear. *Wear*, 261:1253–1264, 2006.

[2] Joao Pombo, Jorge Ambrosio, Manuel Pereira, Roger Lewis, Rob Dwyer-Joyce, Caterina Ariaudo, and Naim Kuka. Development of a wear prediction tool for steel railway wheels using three alternative wear functions. *Wear*, 20:327–358, 2011.

[3] E. Meli, S. Falomi, M. Malvezzi, and A. Rindi. Determination of wheel - rail contact points with semianalytic methods. *Multibody System Dynamic*, 20:327–358, 2008.

[4] J. J. Kalker. *Three-dimensional Elastic Bodies in Rolling Contact*. Kluwer Academic Publishers, Dordrecht, Netherlands, 1990.

[5] S. Iwnicki. *The Manchester Benchmarks for Rail Vehicle Simulators*. Swets and Zeitlinger, Lisse, Netherland, 1999, 2008.

[6] M. Ignesti, M. Malvezzi, L. Marini, E. Meli, and A. Rindi. Development of a wear model for the prediction of wheel and rail profile evolution in railway systems. *Wear*, 284-285:1–17, 2012.

[7] EN 15313: Railway applications — In-service wheelset operation requirements — In-service and off-vehicle wheelset maintenance, 2010.

[8] C. Esveld. *Modern Railway Track*. Delft University of Technology, Delft, Netherland, 2001, 1985.